J. Cell. Mol. Med. Vol 14, No 9, 2010 pp. 2281-2291

MFTZ-1 reduces constitutive and inducible HIF-1α accumulation and VEGF secretion independent of its topoisomerase II inhibition

Mei Dai [a], Ze-Hong Miao [a, *], Xuan Ren [a], Lin-Jiang Tong [a], Na Yang [a], Ting Li [a], Li-Ping Lin [a], Yue-Mao Shen [b], Jian Ding [a, *]

[a] Division of Anti-tumor Pharmacology, State Key Laboratory of Drug Research, Shanghai Institute of Materia Medica, Chinese Academy of Sciences, Shanghai, P.R. China
[b] The State Key Laboratory of Phytochemistry and Plant Resources in West China, Kunming Institute of Botany, Chinese Academy of Sciences, Kunming, P.R. China

Received: December 10, 2008; Accepted: May 8, 2009

Abstract

The macrolide compound MFTZ-1 has been identified as a novel topoisomerase II (Top2) inhibitor with potent *in vitro* and *in vivo* anti-tumour activities. In this study, we further examined the effects of MFTZ-1 on hypoxia-inducible factor-1α (HIF-1α) accumulation, vascular endothelial growth factor (VEGF) secretion and angiogenesis. MFTZ-1 reduced HIF-1α accumulation driven by hypoxia or growth factors in human cancer cells. Mechanistic studies revealed that MFTZ-1 did not affect the degradation of HIF-1α protein or the level of HIF-1α mRNA. By contrast, MFTZ-1 apparently inhibited constitutive and inducible activation of both phosphatidylinositol-3-kinase (PI3K)-Akt and p42/p44 mitogen-activated protein kinase (MAPK) pathways. Further studies revealed that MFTZ-1 abrogated the HIF-1α-driven increase in VEGF mRNA and protein secretion. MFTZ-1 also lowered the basal level of VEGF secretion. The results reveal an important feature that MFTZ-1 can reduce constitutive, HIF-1α-independent VEGF secretion and concurrently antagonize inducible, HIF-1α-dependent VEGF secretion. Moreover, MFTZ-1 disrupted tube formation of human umbilical vein endothelial cells (HUVECs) stimulated by hypoxia with low-concentration serum or by serum at normoxia, and inhibited HUVECs migration at normoxia. MFTZ-1 also prevented microvessel outgrowth from rat aortic ring. These data reflect the potent anti-angiogenesis of MFTZ-1 under different conditions. Furthermore, using specific small interfering RNA targeting Top2α or Top2-defective HL60/MX2 cells, we showed that MFTZ-1 affected HIF-1α accumulation and HUVECs tube formation irrelevant to its Top2 inhibition. Taken together, our data collectively reveal that MFTZ-1 reduces constitutive and inducible HIF-1α accumulation and VEGF secretion possibly *via* PI3K-Akt and MAPK pathways, eliciting anti-angiogenesis independently of its Top2 inhibition.

Keywords: MFTZ-1 • HIF-1α • VEGF • angiogenesis • topoisomerase II inhibitor

Introduction

Hypoxia-inducible factor-1α (HIF-1α) is involved in tumour angiogenesis, metastasis and promotes tumour growth by regulating gene transcription. Moreover, HIF-1α overexpression is an important prognostic factor in malignant tumour development. These features make it an attractive target of new cancer therapeutics [1, 2].

Various factors control the cellular levels of HIF-1α protein [2, 3]. The intracellular oxygen pressure is a major regulator of HIF-1α protein degradation. At normoxia, hydroxylation of HIF-1α by prolyl hydroxylases, which are inhibited at hypoxia, facilitates its proteasome-dependent degradation. Consequently, the protein HIF-1α is almost undetectable in most normoxic tumour cells whereas hypoxia enhances its accumulation [4]. In addition, growth factors such as epidermal growth factor (EGF) and insulin-like factor (IGF) can stimulate HIF-1α protein production, principally through translation promotion *via* both phosphatidylinositol-3-kinase (PI3K)-Akt and p42/p44 mitogen-activated protein kinase (MAPK) pathways and their downstream translation factors including 4EBP1 and p70s6k [5–7]. Noticeably, hypoxia and overactivation of both PI3K-Akt and MAPK pathways occur commonly in solid tumours.

*Correspondence to: Ze-Hong MIAO or Jian DING,
Division of Anti-tumor Pharmacology,
State Key Laboratory of Drug Research,
Shanghai Institute of Materia Medica,
Chinese Academy of Sciences, Shanghai 201203, P.R. China.
Tel.: +86-21-50805897
Fax: +86-21-50806722
E-mail: zhm@jding.dhs.org; jding@mail.shcnc.ac.cn

doi:10.1111/j.1582-4934.2009.00822.x

Vascular endothelial growth factor (VEGF) is a strong proangiogenic factor that is essential to the initiation and progression of tumour angiogenesis including growth and migration of endothelial cells and tube formation [8]. The VEGF gene is one of the major transcription target genes of HIF-1α, and on the other hand VEGF expression can also be promoted upon activation of both PI3K-Akt and MAPK pathways. As a result, there are high levels of basal VEGF secretion in solid tumours, even at normoxic conditions [9–12].

In this study, we demonstrate that the novel topoisomerase II (Top2) inhibitor 4-ethyl-2,5,11-trimethyl- 4,13,19,20-tetraoxa-tricyclo [14.2.1.1(7,10)] eicosane-3,12- dione (MFTZ-1) (Fig. S1) [13] blocked both constitutive and inducible HIF-1α accumulation and in particular, inhibited VEGF secretion in HIF-1α-dependent and -independent manners. All these are further identified to be because of arresting both the PI3K-Akt and MAPK pathways. Consequently, MFTZ-1 combated angiogenic events in all examined conditions, which was independent of its Top2-targeted effect.

Materials and methods

Compounds and antibodies

MFTZ-1 was isolated from an endophyte streptomyces sp.Is9131 of M. hookeri as previously reported [14] and its purity is greater than 95%. The compound was dissolved in dimethylsulfoxide (DMSO) at 0.01 M and stored at –80°C. Just prior to each experiment, it was diluted with sterile normal saline to desired concentrations. The final DMSO concentration did not exceed 0.01% (v/v). LY294002 and U0126 were purchased from Sigma-Aldrich (St. Louis, MO, USA) and epoxomycin and MG132 were obtained from Merck (Whitehouse Station, NJ, USA). The primary antibody for HIF-1α was purchased from the BD Transduction Laboratories (San Jose, CA, USA). The primary antibodies for p-Erk (#9101), Erk (#9102), p-Akt (#9272), Akt (#9271), p-4EBP1 (#9455) and p-p70S6K (#9206) were purchased from Cell Signaling Technology (Danvers, MA, USA), respectively. The primary antibody for Top2α was purchased from Santa Cruz Biotechnology (Santa Cruz, CA, USA). Second antibodies for rabbit IgG and mouse IgG were from Sigma-Aldrich.

Cell culture

Human breast cancer MDA-MB-231 and MDA-MB-468 cells, colon cancer HCT116 cells, melanoma A375 cells, promyelocytic leukaemia HL-60 and the mitoxantrone-resistant variant HL-60/MX2, cervical cancer HeLa cells and non-small cell lung cancer A549 cells were obtained from the American Type Culture Collection (ATCC, Manassas, VA, USA). Cells were normally cultured with ATCC-required medium in a humidified atmosphere with 5% CO_2 incubator at 37°C, except MDA-MB-231 cultured in an atmosphere incubator at 37°C (referred to as normoxic conditions). Hypoxia treatment was performed by putting cells in a CO_2 Water Jacketed Incubator (Model 3110 series, Thermo Forma, Waltham, MA, USA) filled with a mixture of 1% O_2, 5% CO_2 and 94% nitrogen. Human umbilical vein endothelial cells (HUVECs) were isolated from human umbilical cord vein by 0.1% type I collagenase digestion at 37°C for 12 min. and identified with the specific endothelial cell marker von Willebrand factor monoclonal antibody (BD Biosciences, San Jose, CA, USA) by indirect immunofluorescence. HUVECs were grown in M199 medium supplemented with 20% fetal bovine serum (FBS), 30 μg/ml endothelial cell growth supplement (ECGS, Sigma), and 10 ng/ml EGF, 100 units/ml penicillin, and 100 μg/ml streptomycin (Life Technologies). The cells at three to six passages were used in the experiments [15].

Western blotting

Eighty per cent confluenced cells (5×10^5 cells/well) were treated with 0.008 μM to 1 μM MFTZ-1 and/or other agents for the indicated times at hypoxic or normoxic conditions. The cells were collected and lysed in 1 $\times$ SDS gel loading buffer [50 mM Tris-HCl (pH 6.8), 100 mM DTT, 2% SDS, 0.1% bromphenol blue, 10% glycerol], and then boiled for 10–15 min. The same amounts of cell lysates were resolved on 10% SDS polyacrylamide gels, and the proteins were electrotransferred to Hybond-C nitrocellulose membranes (Amersham, Buckinghamshire, UK). The blots were incubated with the indicated primary antibodies, then washed and incubated with the appropriate horseradish peroxidase-conjugated secondary antibodies. Immunoreactivity was visualized using the ECL Plus Western Blotting Detection System (GE Healthcare, Buckinghamshire, UK).

Conditioned medium and ELISA for VEGF

MDA-MB-231 cells were seeded in a six-well plate at a density of 5×10^5 cells per well in L-15 medium supplemented with 10% FBS and 2 mM glutamine. After attachment, the medium was replaced with 1 ml per well of fresh medium, and the cells were treated with MFTZ-1 (0.008, 0.04, 0.2 and 1 μM) or vehicle (0.01% DMSO), and then subjected to hypoxia or normoxia for 16 hrs. Cell supernatants were collected, clarified by centrifugation at 300 $\times$ *g* for 5 min., and stored at –20°C. Simultaneously, cell pellets were harvested by trypsinization, and cell number was calculated with the Z1 Cell Counter (Beckman, Miami, FL, USA). The amount of VEGF in the supernatant was determined with a VEGF-ELISA kit (R&D Systems, Minneapolis, MN, USA) according to the manufacture's instructions. VEGF was calculated as picograms of VEGF protein per millilitre of medium per 105 cells. The figure shown VEGF secretion was expressed as fold-increase, and the baseline was the VEGF concentration of control, respectively [15, 16].

Reverse transcription-PCR (RT-PCR) and quantitative real-time RT-PCR

After treatment of MDA-MB-231 (5 x10^5 cells per well) with MFTZ-1 or vehicle (0.01% DMSO) at hypoxia or normoxia for 6 hrs, total RNA was isolated using the TRIzol reagent (Invitrogen, Carlsbad, CA, USA) according to the manufacturer's instructions. RNA yield and purity were assessed by the spectrophotometric analyses. Total RNA (1 μg) from each sample was subjected to reverse transcription with random hexamer, deoxynucleoside triphosphates and Moloney murine leukaemia virus reverse transcriptase in a total reaction volume of 25 μl PCR was performed on cDNA with TaqDNA polymerase, de-oxynucleoside triphosphate, and the corresponding primers. The following PCR primers synthesized by the Shanghai Research Center of Biotechnology, Chinese Academy sciences were used: Sense:5′-CCC CAG ATT CAG GAT CAG ACA-3′ and antisense: 5′-CCA TCA TGT TCC ATT TTT CGC-3′ for HIF-1α [15] Sense: 5′-TGA CGG GGT CAC CCA CAC TGT GCC CATC-3′ and antisense: 5′-CTA GAA GCA TTT GCG GTC

GAC GAT GGA GGG-3′ for β-Actin [17]. An aliquot of each reaction mixture was analysed by electrophoresis on a 1.5% agarose gel. After being stained with ethidium bromide, the gel was photographed using GeneSnap Version 6.00 software (Syngene, Cambridge, England). The sequence for real-time PCR was: for HIF-1α: 5′-CTC AAA GTC GGA CAG CCTCA-3′ (sense) and 5′-CCC TGC AGT AGG TTT CTG CT-3′ (antisense); for β-Actin: Sense 5′-TGA CGG GGT CAC CCA CAC TGT GCC CATC-3′ and antisense: 5′-CTA GAA GCA TTT GCG GTC GAC GAT GGA GGG-3′ [17]; for VEGF: 5′-TCT TCA AGC CAT CCT GTG TG-3′ (sense) and 5′-TCT CTC CTA TGT GCT GGCCT-3′ (antisense) [18]. The quantitative real-time RT-PCR was performed by TAKARA SYBR Premix EX Taq™. The reaction mixtures containing SYBR Green were composed following the manufacturer's protocol. The cycling program was 95°C 10 sec, 95°C 5 sec and 60°C 30 sec, followed by 39 cycles.

Small interference RNA (siRNA) transfection

siRNA duplexes for Top2α RNA (sense: GGUAUUCCUGUUGUUGAAC) [19] and the HIF-1α siRNA (sense 5′-CUG AUG ACC AGC AAC UUG AdTdT-3′) [20] were synthesized by Shanghai GenePharma Co., Ltd. Transfection was done with Oligofectamine (Invitrogen) according to the manufacturer's instructions. Briefly, MDA-MB-231 cells were seeded into six-well plates and grown to 50–70% confluence before transfection. 100 μl OPTIMEM (Invitrogen) and 5 μl Oligofectamine were pre-incubated for 5 min. at room temperature. Then Oligofectamine were added to 4–5 μl of 20 μM siRNA (final concentrations of 80–100 nM) in 100 μl OPTIMEM and incubated for 20 min. at room temperature to allow complexes formation. The cells were rinsed with OPTIMEM to remove serum and incubated with the oligonucleotide duplexes in a total volume of 1 ml for 4–6 hrs at 37°C. Serum was then added back to the culture and the cells were incubated for the indicated time before starting an experiment.

Tube formation assays

Tube formation of HUVECs was conducted to assay *in vitro* angiogenesis [21]. Briefly, a 96-well plate was coated with 60 μl of Matrigel (Becton Dickinson Labware, San Jose, CA, USA), which was allowed to solidify at 37°C for 1 hr. HUVECs (1×10^4 cells per well) were seeded on the Matrigel and cultured in M199 medium containing different concentrations of MFTZ-1 (0.008, 0.04, 0.2, and 1 μM) or control [0.05% DMSO (v/v)] for 6 hrs. The enclosed networks of complete tubes from five randomly chosen fields were counted and photographed under a microscope (IX70, Olympus, Tokyo, Japan). The inhibition rate of tube formation was calculated by counting the junction (formed by ≥ 3 branch) number and using the following formula: [1-(Junctions MFTZ-1/Junctions control)] ×100%. MFTZ-1 shows little cytotoxicity to HUVECs at the same conditions (data not shown).

To do hypoxia-induced tube formation assays, the plates were coated with 60 μl growth factor-reduced Matrigel at a concentration of 1 mg/ml (BD Biosciences). HUVECs (1.2×10^4 cells per well) suspended with 0.5% FBS M199 medium were added to the Matrigel-coated plates in a final volume of 100 μl [22].

Endothelial cell migration assays

HUVECs migration assays [23] were performed in a Transwell Boyden Chamber (Corning Inc., Corning, NY, USA) using a polycarbonate filter with a pore size of 8.0 μm coated with a 1% gelatin as previously reported.

Aortic ring assays

The aortas were harvested from 6-week-old Sprague-Dawley rats and flushed with M199 using a 21-gauge syringe. Each aorta was sliced into 1 mm slices, placed in 96-well plates containing 60 μl Matrigel, and incubated for 1 hr at 37°C to promote gelling. The aortic rings were fed with M199 with or without various concentrations of MFTZ-1 and photographed on day 6 [24].

Results

MFTZ-1 reduces the cellular accumulation of HIF-1α protein

Our previous study shows that MFTZ-1 has an averaged IC_{50} of 0.99 μM for the exposure duration of 72 hrs in MDA-MB-231 cells [13]. In this study, we found MFTZ-1 to be non- to sub-cytotoxic (growth inhibition <20% *vs* control) to MDA-MB-231 cells in the range of 0.008 μM to 1 μM for 6 hrs and 16 hrs (data not shown). To examine whether MFTZ-1 decreases the level of cellular HIF-α protein, we used these concentrations of the compound to treat human cancer cells under various conditions. When human breast cancer MDA-MB-231 cells were exposed to hypoxia (1% O_2), the level of HIF-1α protein first rose, peaked at the time-point of 6–16 hrs, and then came down (Fig. 1A). Treatment of the cells with MFTZ-1 in hypoxia led to concentration-dependent reduction of cellular HIF-1α protein (Fig. 1B). Similarly, MFTZ-1 also abrogated the accumulation of HIF-1α protein driven by the growth factors EGF (Fig. 1C), which are known to stimulate the expression of HIF-1α protein [5, 6, 25]. Moreover, the levels of HIF-1α protein at hypoxic conditions were diminished by MFTZ-1 in a panel of tumour cell lines with different tissues of origin including breast cancer MDA-MB-468, colon cancer HCT-116, lung cancer A549, melanoma A375 and cervical cancer HeLa cell lines (Fig. 1D). In addition, MFTZ-1 was not revealed to inhibit HIF-2α in SKBr3 and 786-O cells (Fig. S4; HIF-2α was undetectable in MDA-MB-231 cells under the same condition). All these substantiate a universal reduction of HIF-1α protein induced by MFTZ-1 under the complicated conditions including tumour cells with different tissues of origin, normoxia, hypoxia, and stimulation with growth factors, most of which occur in the human body.

MFTZ-1 affects neither proteasome-mediated degradation nor transcription of HIF-1α

The ubiquitin-proteasome system is critical for regulating the level of cellular HIF-1α protein in response to the change in oxygen pressure [4, 26]. To examine whether MFTZ-1 down-regulates HIF-1α protein *via* accelerating its proteasome-mediated degradation, we used two selective proteasome inhibitors MG-132 and

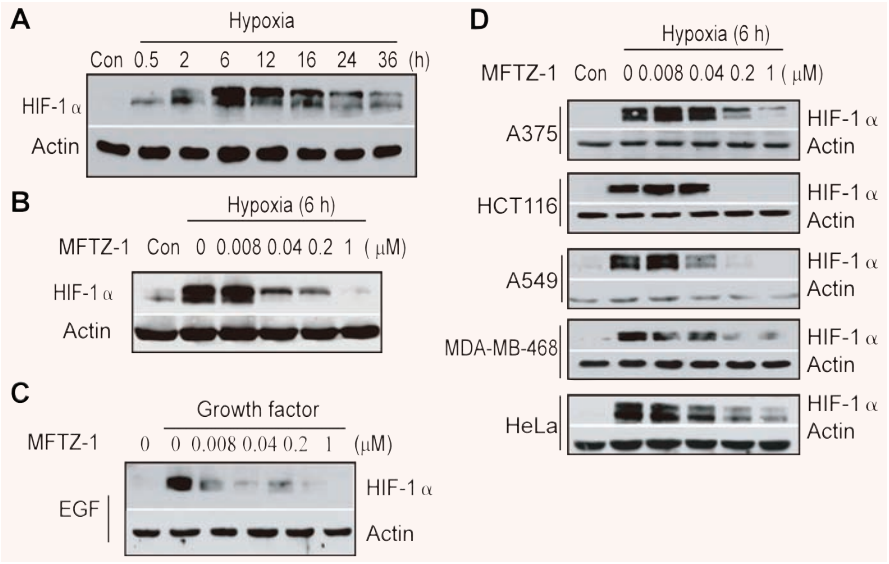

Fig. 1 MFTZ-1 decreases HIF-1α protein accumulation. MDA-MB-231 cells were exposed to hypoxia for the indicated times (**A**), to hypoxia and gradient concentrations of MFTZ-1 for 6 hrs (**B**) and to pre-starved MDA-MB-231 cells were exposed to the indicated concentrations of MFTZ-1 for 4 hrs after stimulated by epidermal EGF (50 ng/ml) for 4 hrs at normoxia (**C**). (**D**) HC T116, A375, A549, MDA-MB-468 and HeLa cells were treated with the indicated concentrations of MFTZ-1 at hypoxia for 6 hrs. Then the cells were collected and detected for HIF-1α and β-Actin by Western blotting. All data shown were representative of three independent experiments.

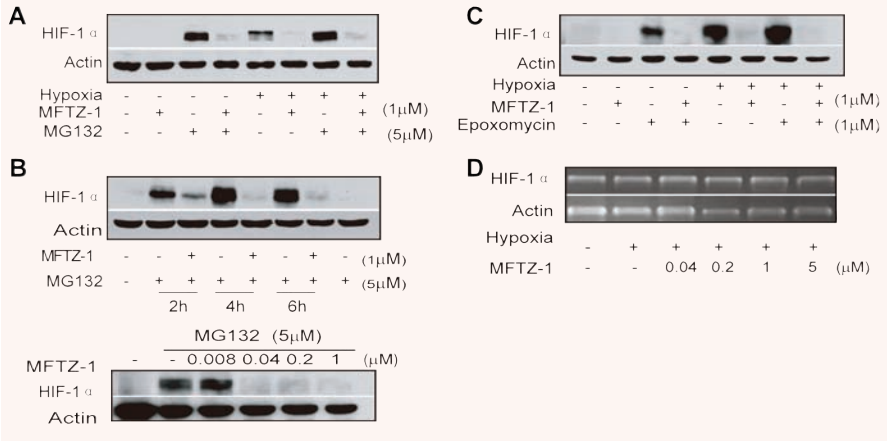

Fig. 2 MFTZ-1 does not accelerate HIF-1α protein degradation or decrease the level of HIF-1α mRNA. MDA-MB-231 cells were treated with MFTZ-1 together with MG132 (**A** and **B**) or epoxomycin (**C**) under the indicated conditions. Then, the cells were collected and detected for HIF-1α and β-Actin by Western blotting. (**D**) MDA-MB-231 cells were treated with the indicated concentrations of MFTZ-1 at hypoxia for 6 hrs. Then the total RNA was extracted and RT-PCR analyses were done to detect the level of HIF-1α mRNA. Data shown were representative of three independent experiments.

epoxomycin to block the function of the proteasome pathway in MDA-MB-231 cells. Although both of the inhibitors increased the accumulation of HIF-1α protein at either normoxic or hypoxic conditions, neither of them reversed the MFTZ-1-triggered decrease of HIF-1α protein (Fig. 2A–C). Further RT-PCR analyses showed that MFTZ-1 did not decrease the level of HIF-1α mRNA (Fig. 2D). The results indicate that MFTZ-1 reduces the level of HIF-1α protein not because of interfering with the HIF-1α protein degradation or the transcription of HIF-1α mRNA.

MFTZ-1 inhibits constitutive and inducible activation of both PI3K-Akt and MAPK pathways

Both the PI3K-Akt pathway [5, 25, 27, 28] and the MAPK pathway [6, 29] have been recently shown to control the translation of HIF-1α. To address whether PI3K-Akt and MAPK pathways involve the MFTZ-1-driven events, we first introduced both the PI3K inhibitor LY294002 (40 μM) and the MEK inhibitor U0126 (10 μM) into the MDA-MB-231 cells which Akt and p44/42 MAPK were constitutively activated and not influenced by the hypoxia. Of note, the introduction of either LY294002 or U0126 was capable of simultaneously preventing the accumulation of HIF-1α protein induced by both hypoxia and growth factors (EGF and IGF-1), accompanied by a reduction in activated Akt and Erk (Fig. S2A and B). All these critical events in hypoxia were imitated in a concentration-dependent way by addition of MFTZ-1 (Fig. 3A). Similarly, MFTZ-1 caused an apparent reduction in phospho-Akt, phospho-Erk, phospho-4EBP1 and phospho-p70s6k in MDA-MB-231 cells stimulated by EGF (Fig. 3B), accompanied by consistent diminution of HIF-1α protein (Fig. 3A and B). All these reveal that MFTZ-1 can inhibit both constitutive and inducible activation of both PI3K-Akt

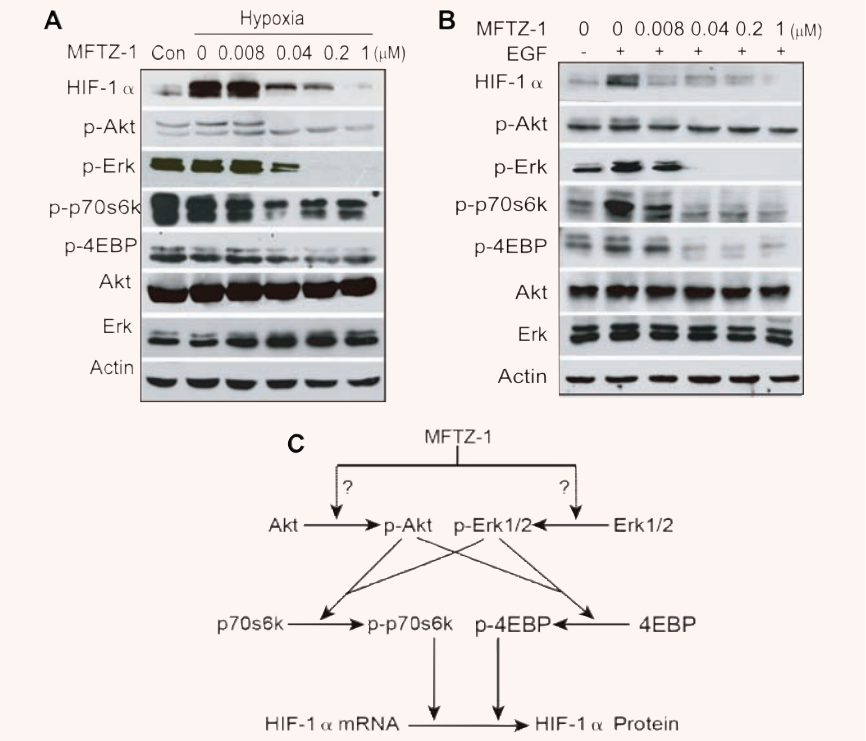

Fig. 3 Effects of MFTZ-1 on Akt and MAPK pathways in MDA-MB-231 cells. Cells were exposed to MFTZ-1 for 6 hrs at hypoxia (**A**), pre-starved MDA-MB-231 cells were exposed to MFTZ-1 for 4 hrs plus pre-stimulation with EGF (50 ng/ml) for 4 hrs at normoxia (**B**) before Western blotting analyses were done for the protein levels of HIF-1α, p-Akt, p-Erk1/2, p-p70s6k and p-4EBP1, Akt and Erk1/2. Data shown were representative of three independent experiments. (**C**) This scheme shows the relationship of Akt, Erk, p70s6k and 4EBP.

and MAPK pathways and may thus repress translation of HIF-1α protein. Additionally, we also found that MFTZ-1 did not affect other important signalling pathways such as JNK, p38MAPK, Hsp90, Hsp70, Hsp27 and NF-κB. (Fig. S3).

Given either the PI3K-Akt pathway or the MAPK pathway is regulated by protein tyrosine kinases [30], it is thus likely that MFTZ-1-driven PI3K-Akt and MAPK-executed events result from its targeting these kinases. For this reason, we detected the impact of MFTZ-1 on several protein tyrosine kinases of concern including EGFR, FGFR1, ErbB2, KDR, c-Kit and c-Src by ELISA [31]. However, MFTZ-1 failed to significantly inhibit any of those tyrosine kinases activities (Table S1).

MFTZ-1 concurrently abrogates both inducible HIF-1α-dependent and constitutive HIF-1α-independent VEGF secretion

To detect whether the reduction of HIF-1α protein by MFTZ-1 changes the expression of HIF-1α-targeted VEGF gene, we used real-time RT-PCR to measure the levels of VEGF mRNA in MFTZ-1-treated MDA-MB-231 cells at hypoxia. The result showed that the hypoxia-induced enhancement of VEGF mRNA was reversed by MFTZ-1 (Fig. 4A).

Next, we examined the effect of MFTZ-1 on VEGF secretion. Hypoxia (1% O_2) alone was noted to enhance the amount of VEGF secretion by 40% as compared with that in normoxia, which was in turn completely reversed by MFTZ-1 even at a concentration as low as 0.04 μM. With the concentrations increasing, VEGF secretion progressively decreased even down to 40% of the normoxic baseline level (Fig. 4A). The data suggest that MFTZ-1 abrogates VEGF secretion in both HIF-1α-dependent and -independent manners.

To confirm the HIF-1α independency of the MFTZ-1-induced decrease in VEGF secretion, we further used specific HIF-1α siRNA to knockdown the expression of HIF-1α (Fig. 4B). At normoxia, either treatment with HIF-1α siRNA or MFTZ-1 alone or treatment with MFTZ-1 after HIF-1α siRNA transfection caused no change in VEGF mRNA in MDA-MB-231 cells (Fig. 4C). However, MFTZ-1 dramatically blocked VEGF secretion regardless of the presence of specific HIF-1α siRNA, although HIF-1α siRNA alone did not reduce such secretion (Fig. 4C). Noticeably, at hypoxia, HIF-1α siRNA prevented the increase in the VEGF secretion driven by hypoxia (Fig. 4A and D), but did not rescue the reduction of the VEGF secretion caused by MFTZ-1 (Fig. 4D). All these substantiate that MFTZ-1 can antagonize inducible, HIF-1α-dependent VEGF secretion and concurrently reduce constitutive, HIF-1α-independent VEGF secretion.

MFTZ-1 combats angiogenesis both *in vitro* and *ex vivo*

Previous reports show that compounds capable of reducing HIF-1α accumulation and VEGF secretion simultaneously inhibit

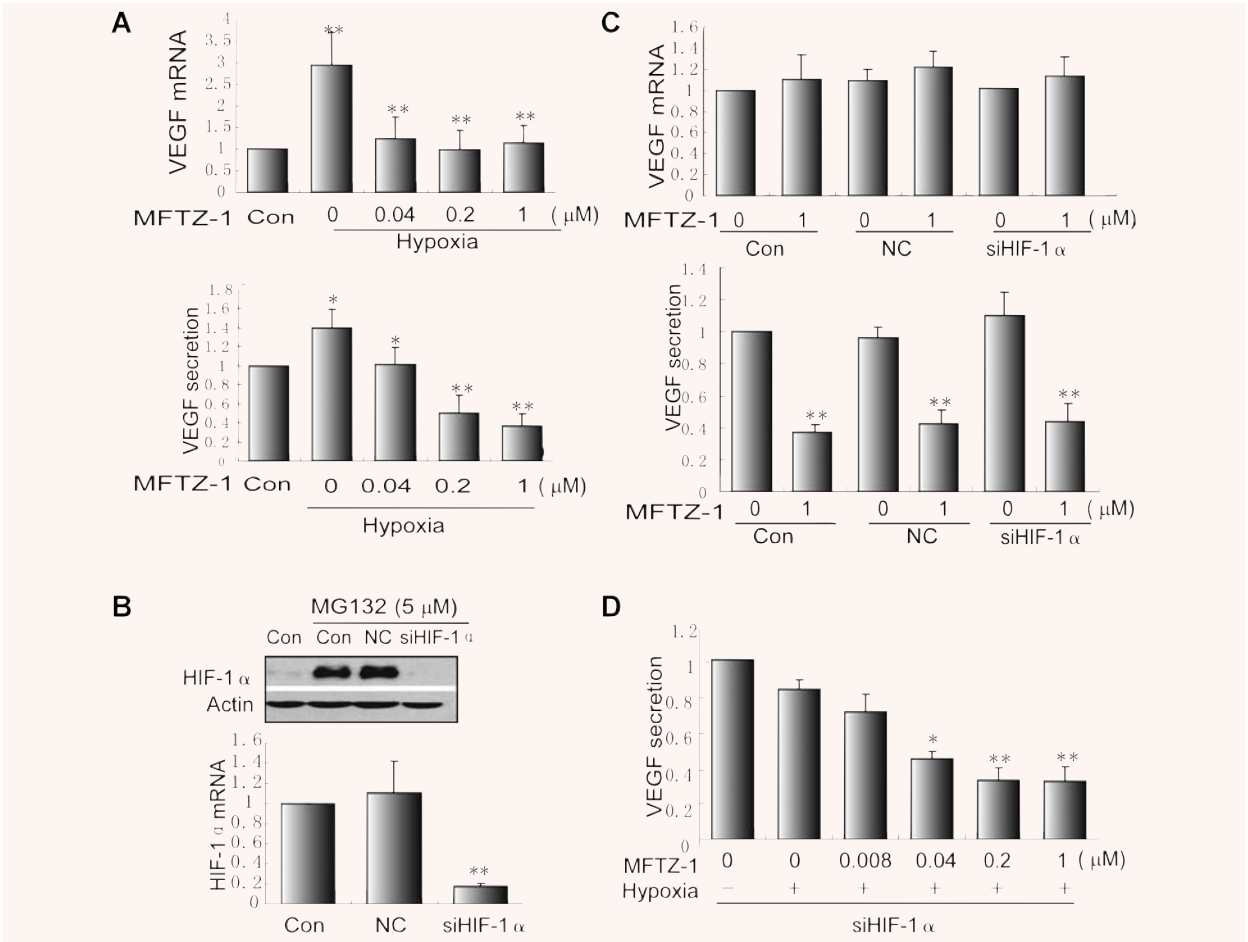

Fig. 4 MFTZ-1 decreases VEGF secretion in MDA-MB-231 cells. (**A**) MFTZ-1 inhibited hypoxia-induced VEGF gene transcription (upper) and VEGF protein secretion (lower) in MDA-MB-231 cells. The cells were treated with the indicated concentrations of MFTZ-1 at hypoxia for 6 hrs (VEGF transcription) or 16 hrs (VEGF secretion). Then total RNA was isolated for VEGF transcription analyses by real-time PCR; or cell supernatants were collected and measured for VEGF levels by ELISA. (**B**) HIF-1α was silenced with 80 nM specific HIF-1α siRNA (siHIF-1α) in both mRNA (lower) and protein (upper) levels. HIF-1α protein was detected by Western blotting in MDA-MB-231 cells transfected with negative control (NC) or siHIF-1α duplexes. Twenty-four hours after transfection, cells were treated with or without MG132 for 4 hrs. Real-time RT-PCR was done to analyse the level of HIF-1α mRNA in MDA-MB-231 cells 24 hrs after transfection. (**C**) Specific down-regulation of HIF-1α with 80 nM siHIF-1α did not affect the effects of MFTZ-1 on VEGF transcription (upper) and secretion (lower) at normoxia. MDA-MB-231 cells were transfected with siHIF-1α or NC for 40 hrs. In the last 16 hrs of the transfection, the cells were treated with or without MFTZ-1. Then real-time RT-PCR and ELISA assays were done separately for detection of VEGF transcription and secretion. (**D**) Silencing HIF-1α (80 nM siHIF-1α) removed the hypoxia-induced increment of VEGF secretion, and MFTZ-1 reduced VEGF secretion of the siHIF-1α-transfected MDA-MB-231 cells at hypoxia. Cells were transfected with siHIF-1α for 40 hrs. In the last 16 hrs of the transfection, the cells were treated with or without MFTZ-1 at hypoxia. Then ELISA assays were done for detection of VEGF secretion. The data represent three independent experiments. Student's t-tests were performed to compare hypoxic control with normoxic control and each drug treatment with the hypoxic control in (**A**), to compare all other treatment with control in (**B**), (**C**) and (**D**). The significance was indicated as * for $P < 0.05$ and ** for $P < 0.01$.

angiogenesis directly [15, 32]. Also hypoxia-induced HIF-1α is essential for hypoxia-induced angiogenesis, especially tube formation [33]. To further investigate whether MFTZ-1 has anti-angiogenic effects, we employed a series of standard angiogenesis models. In the HUVEC tube formation assay, MFTZ-1 potently suppressed the cord formation of HUVEC stimulated by hypoxia (Fig. 5A) or serum at normoxia (Fig. 5B) at a concentration as low as 0.04 μM (Fig. 1). In term of endothelial migration, HUVEC chemotactically (20% FBS) moved from the upper side to the lower side of the membrane in the Boyden chamber [15]. MFTZ-1 repressed this process in a

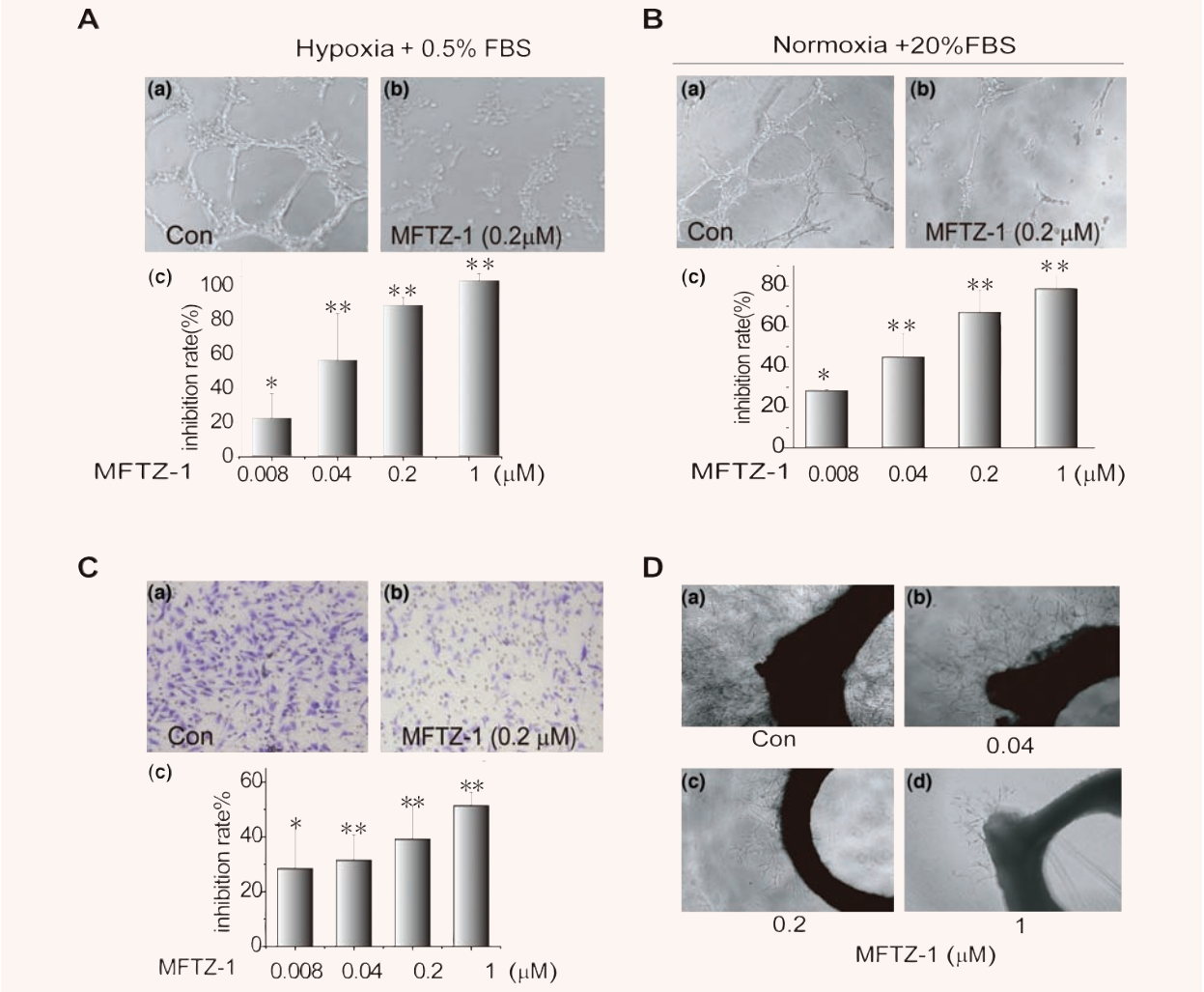

Fig. 5 MFTZ-1 inhibits angiogenesis. (**A**) MFTZ-1 inhibited hypoxia-induced HUVECs tube formation. HUVEC cells (1.2×10^4) were incubated in M199 medium supplemented with 0.5% FBS at hypoxia for 10 hrs to form complete tubes. Treatment with MFTZ-1 abrogated hypoxia-induced tube formation. (a) Control; (b) 0.2 μM MFTZ-1; (c) inhibition rates of tube formation were calculated as in the section of Materials and Methods. Values were expressed as means; bars, ±S.D., $n = 3$. (**B**) MFTZ-1 inhibited serum-induced HUVECs tube formation. HUVEC cells (1×10^4) were cultured in M199 medium supplemented with 20% FBS at normoxia with or without MFTZ-1. After incubation for 6 hrs at 37°C, capillary networks were photographed and quantified. (a) Control; b. 0.2 μM MFTZ-1; (c) inhibition rates were calculated and expressed as in (**A**). (**C**) HUVEC (5×10^4) cells were cultured in a Transwell Boyden Chamber using a polycarbonate filter with a pore size of 8.0 μm coated with a 1% gelatin in serum-free M199 medium with or without MFTZ-1. For migration detection, 20% FBS were added into the lower chamber. After incubation for 6 hrs at 37°C, the migrated cells were photographed and quantified as described in Materials and Methods. (a) Control; (b) 0.2 μM MFTZ-1; (c) inhibition rates of HUVEC migration by MFTZ-1. Values are expressed as means; bars, ±S.D., $n = 3$. (**D**) MFTZ-1 inhibited new microvessel outgrowth arising from rat aortic ring. Data shown were representative of three independent experiments. Student's t-tests were conducted to compare drug treatment with each control, respectively, significance was indicated as * for $P < 0.05$ and ** for $P < 0.01$.

concentration-dependent manner (Fig. 5C). An *ex vivo* model further demonstrated that MFTZ-1 prominently prevented new microvessel outgrowth arising from rat aortic ring (Fig. 5D). All the experiments were manipulated with MFTZ-1 at its sub-cytotoxic concentration regimens (0.008 μM to 1 μM), the concentration of which is 10-fold lower than required for its targeting Top2 [13].

MFTZ-1 reduces HIF-1α protein and suppresses angiogenesis independent of its Top2 inhibition

MFTZ-1 has been demonstrated to be a novel Top2 inhibitor [13]. To examine whether MFTZ-1-triggered reduction of HIF-1α protein is related to its Top2 inhibition, we employed specific siRNA to

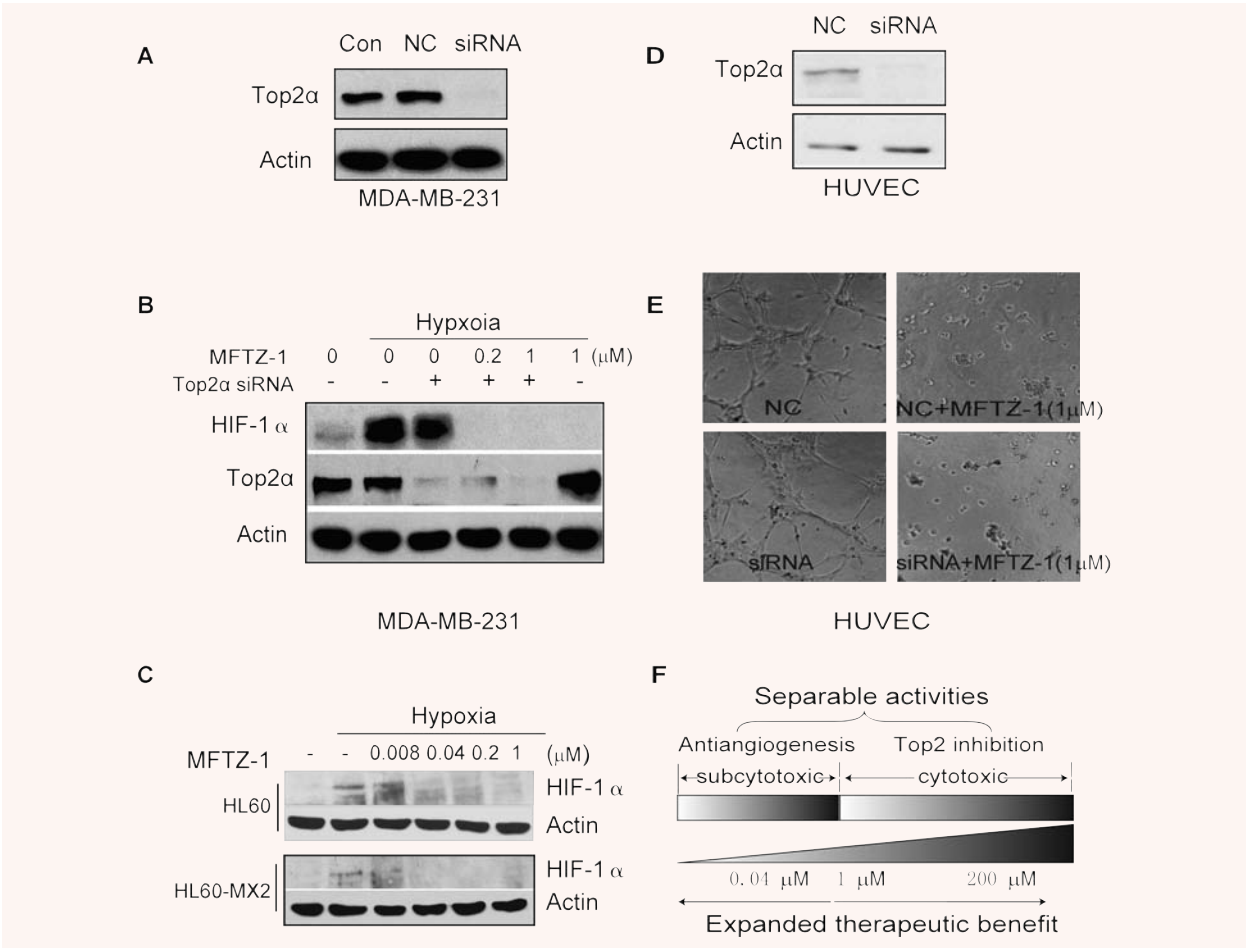

Fig. 6 MFTZ-1 reduces HIF-1α and inhibits tube formation in a Top2-independent manner. (**A**) Transfection efficiency of siRNA targeting Top2α (100 nM) in MDA-MB-231 cells. The cells were collected for Western blotting 36 hrs after transfection. (**B**) Silencing Top2α did not affect the MFTZ-1-mediated decrease in HIF-1α protein. After transfection with mock or Top2α siRNA for 36 hrs, the cells were moved to a hypoxia incubator and continued to be incubated with or without MFTZ-1(0.2, 1 μM) for 4 hrs before Western blotting was done. (**C**) MFTZ-1 reduced HIF-1α protein accumulation in HL60 and functional Top2-defective HL60/MX2. Cells were treated with indicated concentration of MFTZ-1 at hypoxia for 6 hrs. Then the cells were lysed and detected for HIF-1α and β-Actin by Western blotting. Data shown were representative of three independent experiments. (**D**) Transfection efficiency of Top2α (100 nM) siRNA in HUVEC cells. The cells were collected for Western blotting 36 hrs after transfection. (**E**) Silencing Top2α did not affect the MFTZ-1-mediated inhibition of HUVEC tube formation. After transfection with mock or Top2α siRNAs for 36 hrs, HUVEC cells (1.2×10^4) in M199 medium with or without 1 μM MFTZ-1 were added to matrigel and continued to be incubated for 8 hrs at 37°C. Capillary networks were photographed. Data shown were representative of three independent experiments. (**F**) The separable activities of MFTZ-1 on angiogenesis and Top2.

silence Top2α in MDA-MB-231 cells (Fig. 6A). Disruption of Top2α neither eliminated the hypoxia-induced HIF-α protein accumulation, nor reversed the MFTZ-1-mediated decline of HIF-α protein accumulation (Fig. 6B).

The result was further confirmed in HL60/MX2 cells that are defective for functional Top2 (*versus* the parental HL60 cells) [34, 35] (Fig. 6C). Furthermore, silencing Top2α in endothelial HUVEC cells did not exert obviously detectable effects on the ability of the cells to form microvessel-like tubes or on the suppression of tube formation by MFTZ-1 (Fig. 6D and E). All these collectively indicate that MFTZ-1 decreases the cellular accumulation of HIF-1α protein and inhibits angiogenesis in a Top2-independent fashion.

Discussion

MFTZ-1 (14-Ethyl-2,5,11-trimethyl-4,13,19,20-tetraoxa-tricyclo [14.2.1.1(7,10)]eico- sane-3,12-dione) (Fig. S2), a novel macrolide compound isolated from *Streptomyces sp. Is9131,* displays potent

in vitro and *in vivo* anticancer activities (13). Further study shows that MFTZ-1 functions as a novel non-intercalative Top2 inhibitor *via* binding to the ATPase domain of Top2α, characterized by its strong inhibition on the decatenation and relaxation of Top2α [13]. In this study, MFTZ-1 was further noted to universally block HIF-1α protein accumulation induced by hypoxia and by growth factors EGF in human tumour cell lines originated from different tissues. Moreover, MFTZ-1 antagonized both inducible HIF-1α-dependent and constitutive, HIF-1α-independent VEGF secretion.

In tumours, complicated factors including environmental O_2 concentrations and growth factors control the level of HIF-1α protein [36]. Hypoxia, widely occurring in most solid tumours, increases cellular HIF-1α accumulation mainly *via* blocking O_2-dependent and proteasome-executed degradation [3]. In this current study, both selective proteasome inhibitors MG132 and epoxomycin failed to rescue the MFTZ-1-triggered reduction of HIF-1α accumulation in hypoxic MDA-MB-231 cells, suggestive of the irrelevance to the proteasome-mediated degradation.

PI3K-Akt and MAPK pathways are overactivated in most tumours, which can be further enhanced by growth factors such as EGF and IGF, thus promote the activities of translation factors including p70s6k and 4EBP1, and increase the syntheses of multiple proteins including HIF-1α [7, 37]. In the present study, MFTZ-1 was encouragingly noted to inhibit both constitutive and inducible PI3K-Akt and MAPK pathway activation, reduce the basal and inducible syntheses of HIF-1α protein and consequently remove the increase in HIF-1α protein at normoxia, hypoxia and stimulation by growth factors. All these show that MFTZ-1-driven HIF-1α protein reduction under various conditions may well result from its inhibition on the constitutive and inducible activation of both PI3K-Akt and MAPK pathway.

The impact of MFTZ-1 on VEGF secretion seems much more complicated. On the one hand, HIF-1α functions as a critical transcription factor of the VEGF gene [36]. As such, it is reasonable to believe that the reduction of the inducible HIF-1α-dependent VEGF secretion trigged by MFTZ-1 is likely to be the consequence of HIF-1α reduction, as is evident from the fact that MFTZ-1 removed the inducible increment of VEGF mRNA. And when HIF-1α was knocked down by its siRNA, hypoxia could not induce VEGF secretion. On the other hand, the synthesis of VEGF protein is also under control of the translation factor eIF4E. The mRNA cap-binding protein, eucaryotic initiation factor 4E, is a rate-limiting factor of cap-dependent translation initiation of several proteins including VEGF. Phosphorylation of 4EBP1 promotes the dissociation of 4EBP1 from eIF4E and thus activates eIF4E [38–40]. Our findings that MFTZ-1 inhibits the constitutive activation of both PI3K-Akt and MAPK pathways and thus the phosphorylation of 4EBP1 highly imply that the arrest of MFTZ-1 on the constitutive HIF-1α-independent VEGF secretion is in both PI3K-Akt and MAPK-dependent manner. However, the result that MFTZ-1 failed to inhibit the tested protein tyrosine kinases that function upstream of the PI3K-Akt and MAPK pathways makes the question of how MFTZ-1 targets both these pathways open to be answered.

Dozens of anticancer agents with different anticancer molecular targets have been shown to inhibit HIF-1α by distinct mechanisms such as reducing mRNA levels, protein levels, DNA binding and transactivation of HIF-1α [2]. Most of them are only demonstrated to suppress accumulation or activity of HIF-1α protein at hypoxia. This would be a limited factor for their clinical use because of *in vivo* tumours facing the constantly changing environment. In this study, MFTZ-1 behaved distinctly from others by combating constitutive and inducible HIF-1α accumulation and reducing both inducible HIF-1α-dependent and constitutive HIF-1α-independent VEGF secretion, favouring its promising anti-angiogenic potency under more intractable conditions in cancer therapy.

Recently, a few Top2 inhibitors, including doxorubicin [41] and NSC644221 [42] have been shown to inhibit hypoxia-induced HIF-1α activity; particularly noted that NSC644221 abolishes hypoxia-induced HIF-1α-driven events in a cell type-specific and Top2-dependent manner. Such a potential link between HIF-1α and Top2 arouses our interest. However, the total irrelevance of MFTZ-1-driven HIF-1α-executed settings to its Top2 inhibition suggests that MFTZ-1, in a common sense, has a dual target of anti-angiogenesis and Top2 inhibition. With research giving insights into the structure-based activity of the class of this compound, it is hoped that targeting both anti-angiogenesis and Top2 inhibition in a separable manner might offer more appreciable therapeutic opportunities to the practical benefits (Fig. 6F).

Acknowledgements

This study was supported by the grant (No. 30721005) from the National Natural Science Foundation of China (NSFC). The authors have no conflicting financial interests.

Supporting Information

Additional Supporting Information may be found in the online version of this article:

Methods

ELISA kinase assays

Briefly, 50 μl 10 μM ATP solution diluted in kinase reaction buffer (50 mM HEPES pH 7.4, 20 mM MgCl2, 0.1 mM MnCl2, 0.2 mM Na3VO4, 1 mM DTT) was added to each well. MFTZ-1 in 10 μl buffered saline was added to each reaction well. The kinase reaction was performed in triplicate and initiated by adding purified tyrosine kinase proteins diluted in 40 μl of kinase reaction buffer. After incubation for 60 min. at 37°C, the plate was washed three times, then 100 μl anti-phosphotyrosine (PY99) antibody (1:500,

Santa Cruz, CA, USA) was added and the plate was placed at 37°C for 30 min. After the plate was washed three times, Horseradish peroxidase-conjugated goat antimouse IgG (1:2000, Calbiochem, San Diego, CA, USA) was added and the plate was re-incubated at 37°C for 30 min. The plate was washed, then 100 μl citrate buffer (0.1 M, pH 5.5) containing 0.03% H2O2 and 2 mg/ml o-phenylenediamine was added and the samples were incubated at room temperature until colour emerged. The reaction was terminated by adding 50 μl of 2 M H2SO4, and the plate was read using a multi-well spectrophotometer (VERSAmax™, Molecular Devices, Sunnyvale, CA, USA) at 492 nm. The inhibition rate (%) was calculated with the formula: [1-(A492/A492 control)]×100%.

Western blotting

MDA-MB-231, SKBr3 and 786-O cells were culturedin L-15 and RPMI1640, respectively. After 80% confluence in 6-well plates, cells were treated with the indicated concentrations of MFTZ-1 at hypoxia or nomoxia for 6 hrs. Then the cells were collected and detected for p-JNK (Cell Signaling), JNK (Santa Cruz Biotechnology), p-p38 (Beyond, Shanghai, China), p38 (Beyond), Hsp90 (BD Biosciences), Hsp70 (BD Biosciences), Hsp27 (BD Biosciences), HIF-1α (BD Biosciences), HIF-2α (Boster, Wuhan, China) and β-Actin (Sigma-Aldrich) by Western blotting. All data shown were representative of three independent experiments.

NF-κB immunofluorescence

MDA-MB-231 cells grown on glass cover slips were fixed for 15 min. with 4% paraformaldehyde and then permeabilized for 10 min. with 0.1% TritonX-100. Following subsequent saturation with 3% bovine serum albumin, the cells were incubated with anti-NF-κB (p65) rabbit antibody (1:200, Santa Cruz, USA) overnight. Then, the cells were stained with Alexa Fluor® 488-conjugated secondary antibody (1:200, Invitrogen) for 1 hr. Finally, slides were mounted by VECTASHIELD with DAPI (Vector laboratories, Burlingame, CA, USA) and the cells were imaged by microscopy (Leica, Deerfield, IL, USA). All data shown were representative of three independent experiments.

Table S1 MFTZ-1 does not inhibit c-Kit, EGFR, FGFR, ErbB2, KDR, c-Src kinase activities analysed by biochemical tyrosine kinase assays in cell-free system [23]. The inhibition rate (%) = [1 – ($A_{492}/A_{492\ control}$)] ×100%. The inhibition rate in the table was the averages of three independent experiments. SU11248, GW374, SU5402, PP2 were used as positive control.

Fig. S1 Chemical structure of MFTZ-1

Fig. S2 The PI3K inhibitor LY294002 (**A, B**) and the MEK inhibitor U0126 (**A, B**) suppress Akt and MAPK pathways and the accumulation of HIF-1α protein in MDA-MB-231 cells. (**A**) Cells were treated with 40 μM LY294002 or 10 μM U0126 at hypoxia for 6 hrs before Western blotting analyses. (**B**) Cells were starved for 24 hrs, treated with 40 μM LY294002 or 10 μM U0126 for 4 hrs before stimulation with EGF or IGF for 4 hrs, and then collected for Western blotting.

Fig. S3 MFTZ-1 does not affect JNK and p38MAPK pathways, Hsp family proteins, or the nuclear translocation of NF-κB. (**A**) MDA-MB-231 cells were treated with the indicated concentrations of MFTZ-1 at hypoxia for 6 hrs. Then the cells were collected and detected for Western blotting. (**B**) MDA-MB-231cells were treated with MFTZ-1 in nomoxia, and the other is the same with 'A'. (**C**) MDA-MB-231 cells grown on glass cover slip treated with or without 1 μM MFTZ-1 for 6 hrs were fixed for NF-κB (P65) immunofluorescence. TNFα (10 ng/ml) stimulation for 10 min. was a positive control for NF-κB translocation.

Fig. S4 Effects of MFTZ-1 on HIF-1α *versus* HIF-2α. (**A**) MFTZ-1 decreased HIF-1α dramatically, but had little reduction on HIF-2α protein in SKBr3 breast cancer cells. In 786-O cells, MFTZ-1 also had undetectable effect on HIF-2α protein. (**B**) Densitometry analysis of HIF-1α and HIF-2α levels in SKBr3 cells treated with MFTZ-1. The data were from three independent experiments.

Please note: Wiley-Blackwell are not responsible for the content or functionality of any supporting materials supplied by the authors. Any queries (other than missing material) should be directed to the corresponding author for the article.

References

1. **Giaccia A, Siim BG, Johnson RS.** HIF-1 as a target for drug development. *Nat Rev Drug Discov.* 2003; 2: 803–11.
2. **Semenza GL.** Evaluation of HIF-1 inhibitors as anticancer agents. *Drug Discov Today.* 2007; 12: 853–9.
3. **Ke Q, Costa M.** Hypoxia-inducible factor-1 (HIF-1). *Mol Pharmacol.* 2006; 70: 1469–80.
4. **Stolze IP, Mole DR, Ratcliffe PJ.** Regulation of HIF: prolyl hydroxylases. *Novartis Found Symp.* 2006; 272: 15–25; discussion 25–36.
5. **Fukuda R, Hirota K, Fan F, *et al.*** Insulin-like growth factor 1 induces hypoxia-inducible factor 1-mediated vascular endothelial growth factor expression, which is dependent on MAP kinase and phosphatidylinositol 3-kinase signaling in colon cancer cells. *J Biol Chem.* 2002; 277: 38205–11.
6. **Slomiany MG, Black LA, Kibbey MM, *et al.*** IGF-1 induced vascular endothelial growth factor secretion in head and neck squamous cell carcinoma. *Biochem Biophys Res Commun.* 2006; 342: 851–8.
7. **Treins C, Giorgetti-Peraldi S, Murdaca J, *et al.*** Insulin stimulates hypoxia-inducible factor 1 through a phosphatidylinositol 3-kinase/target of rapamycin-dependent signaling pathway. *J Biol Chem.* 2002; 277: 27975–81.
8. **Ferrara N, Bunting S.** Vascular endothelial growth factor, a specific regulator of angiogenesis. *Curr Opin Nephrol Hypertens.* 1996; 5: 35–44.

9. **Mamane Y, Petroulakis E, LeBacquer O, *et al.*** mTOR, translation initiation and cancer. *Oncogene.* 2006; 25: 6416–22.
10. **Trisciuoglio D, Iervolino A, Zupi G, *et al.*** Involvement of PI3K and MAPK signaling in bcl-2-induced vascular endothelial growth factor expression in melanoma cells. *Mol Biol Cell.* 2005; 16: 4153–62.
11. **Segrelles C, Ruiz S, Santos M, *et al.*** Akt mediates an angiogenic switch in transformed keratinocytes. *Carcinogenesis.* 2004; 25: 1137–47.
12. **Tong Y, Zhang X, Tian F, *et al.*** Philinopside A, a novel marine-derived compound possessing dual anti-angiogenic and anti-tumor effects. *Int J Cancer.* 2005; 114: 843–53.
13. **Xie CY, Zhu H, Lin LP, *et al.*** MFTZ-1, an actinomycetes subspecies derived antitumor macrolide, functions as a novel topoisomerase II poison. *Mol Cancer Ther.* 2007; 6: 3059–70.
14. **Zhao PJ, Fan LM, Li GH, *et al.*** Antibacterial and antitumor macrolides from Streptomyces sp. Is9131. *Arch Pharm Res.* 2005; 28: 1228–32.
15. **Li MH, Miao ZH, Tan WF, *et al.*** Pseudolaric acid B inhibits angiogenesis and reduces hypoxia-inducible factor 1alpha by promoting proteasome-mediated degradation. *Clin Cancer Res.* 2004; 10: 8266–74.
16. **Blancher C, Moore JW, Talks KL, *et al.*** Relationship of hypoxia-inducible factor (HIF)-1alpha and HIF-2alpha expression to vascular endothelial growth factor induction and hypoxia survival in human breast cancer cell lines. *Cancer Res.* 2000; 60: 7106–13.
17. **Zhou J, Schmid T, Frank R, Brune B.** PI3K/Akt is required for heat shock proteins to protect hypoxia-inducible factor 1alpha from pVHL-independent degradation. *J Biol Chem.* 2004; 279: 13506–13.
18. **Ben-Shoshan M, Amir S, Dang DT, *et al.*** 1{alpha},25-dihydroxyvitamin D3 (Calcitriol) inhibits hypoxia-inducible factor-1/vascular endothelial growth factor pathway in human cancer cells. *Mol Cancer Ther.* 2007; 6: 1433–9.
19. **Qin Y, Meng L, Hu C, *et al.*** Gambogic acid inhibits the catalytic activity of human topoisomerase IIalpha by binding to its ATPase domain. *Mol Cancer Ther.* 2007; 6: 2429–40.
20. **Sowter HM, Raval RR, Moore JW, *et al.*** Predominant role of hypoxia-inducible transcription factor (Hif)-1alpha *versus* Hif-2alpha in regulation of the transcriptional response to hypoxia. *Cancer Res.* 2003; 63: 6130–4.
21. **Ashton AW, Yokota R, John G, *et al.*** Inhibition of endothelial cell migration, intercellular communication, and vascular tube formation by thromboxane A(2). *J Biol Chem.* 1999; 274: 35562–70.
22. **Calvani M, Rapisarda A, Uranchimeg B, *et al.*** Hypoxic induction of an HIF-1alpha-dependent bFGF autocrine loop drives angiogenesis in human endothelial cells. *Blood.* 2006; 107: 2705–12.
23. **Zhong L, Guo XN, Zhang XH, *et al.*** TKI-31 inhibits angiogenesis by combined suppression signaling pathway of VEGFR2 and PDGFRbeta. *Cancer Biol Ther.* 2006; 5: 323–30.
24. **Zhao H, Liu H, Chen Y, *et al.*** Oligomannurarate sulfate, a novel heparanase inhibitor simultaneously targeting basic fibroblast growth factor, combats tumor angiogenesis and metastasis. *Cancer Res.* 2006; 66: 8779–87.
25. **Jiang BH, Jiang G, Zheng JZ, *et al.*** Phosphatidylinositol 3-kinase signaling controls levels of hypoxia-inducible factor 1. *Cell Growth Differ.* 2001; 12: 363–9.
26. **Kong X, Alvarez-Castelao B, Lin Z, *et al.*** Constitutive/hypoxic degradation of HIF-alpha proteins by the proteasome is independent of von Hippel Lindau protein ubiquitylation and the transactivation activity of the protein. *J Biol Chem.* 2007; 282: 15498–505.
27. **Laughner E, Taghavi P, Chiles K, *et al.*** HER2 (neu) signaling increases the rate of hypoxia-inducible factor 1alpha (HIF-1alpha) synthesis: novel mechanism for HIF-1-mediated vascular endothelial growth factor expression. *Mol Cell Biol.* 2001; 21: 3995–4004.
28. **Pore N, Jiang Z, Shu HK, *et al.*** Akt1 activation can augment hypoxia-inducible factor-1alpha expression by increasing protein translation through a mammalian target of rapamycin-independent pathway. *Mol Cancer Res.* 2006; 4: 471–9.
29. **Melillo G.** Inhibiting hypoxia-inducible factor 1 for cancer therapy. *Mol Cancer Res.* 2006; 4: 601–5.
30. **Sebolt-Leopold JS, English JM.** Mechanisms of drug inhibition of signalling molecules. *Nature.* 2006; 441: 457–62.
31. **Guo XN, Zhong L, Zhang XH, *et al.*** Evaluation of active recombinant catalytic domain of human ErbB-2 tyrosine kinase, and suppression of activity by a naturally derived inhibitor, ZH-4B. *Biochim Biophys Acta.* 2004; 1673: 186–93.
32. **Kamiyama H, Takano S, Tsuboi K, *et al.*** Anti-angiogenic effects of SN38 (active metabolite of irinotecan): inhibition of hypoxia-inducible factor 1 alpha (HIF-1alpha)/vascular endothelial growth factor (VEGF) expression of glioma and growth of endothelial cells. *J Cancer Res Clin Oncol.* 2005; 131: 205–13.
33. **Tang N, Wang L, Esko J, *et al.*** Loss of HIF-1alpha in endothelial cells disrupts a hypoxia-driven VEGF autocrine loop necessary for tumorigenesis. *Cancer Cell.* 2004; 6: 485–95.
34. **Zhu H, Huang M, Yang F, *et al.*** R16, a novel amonafide analogue, induces apoptosis and G2-M arrest *via* poisoning topoisomerase II. *Mol Cancer Ther.* 2007; 6: 484–95.
35. **Harker WG, Slade DL, Parr RL, *et al.*** Alterations in the topoisomerase II alpha gene, messenger RNA, and subcellular protein distribution as well as reduced expression of the DNA topoisomerase II beta enzyme in a mitoxantrone-resistant HL-60 human leukemia cell line. *Cancer Res.* 1995; 55: 1707–16.
36. **Liao D, Johnson RS.** Hypoxia: a key regulator of angiogenesis in cancer. *Cancer Metastasis Rev.* 2007; 26: 281–90.
37. **Wada-Kiyama Y, Kiyama R.** Periodicity of DNA bend sites in human epsilon-globin gene region. Possibility of sequence-directed nucleosome phasing. *J Biol Chem.* 1994; 269: 22238–44.
38. **Yang SX, Hewitt SM, Steinberg SM, *et al.*** Expression levels of eIF4E, VEGF, and cyclin D1, and correlation of eIF4E with VEGF and cyclin D1 in multi-tumor tissue microarray. *Oncol Rep.* 2007; 17: 281–7.
39. **Dong K, Wang R, Wang X, *et al.*** Tumor-specific RNAi targeting eIF4E suppresses tumor growth, induces apoptosis and enhances cisplatin cytotoxicity in human breast carcinoma cells. *Breast Cancer Res Treat.* 2009; 113: 443–56.
40. **Semenza GL.** Targeting HIF-1 for cancer therapy. *Nat Rev Cancer.* 2003; 3: 721–32.
41. **Duyndam MC, van Berkel MP, Dorsman JC, *et al.*** Cisplatin and doxorubicin repress vascular endothelial growth factor expression and differentially down-regulate hypoxia-inducible factor I activity in human ovarian cancer cells. *Biochem Pharmacol.* 2007; 74: 191–201.
42. **Creighton-Gutteridge M, Cardellina JH 2nd, Stephen AG, *et al.*** Cell type-specific, topoisomerase II-dependent inhibition of hypoxia-inducible factor-1alpha protein accumulation by NSC 644221. *Clin Cancer Res.* 2007; 13: 1010–8.